



# Anomaly detection of cooling fan and fault classification of induction motor using Mahalanobis–Taguchi system



Xiaohang Jin, Tommy W.S. Chow\*

Centre for Prognostics and System Health Management, City University of Hong Kong, Hong Kong, China  
Department of Electronic Engineering, City University of Hong Kong, Hong Kong, China

## ARTICLE INFO

### Keywords:

Anomaly detection  
Cooling fan  
Fault classification  
Induction motor  
Mahalanobis–Taguchi system  
Vibration signal

## ABSTRACT

A health index, Mahalanobis distance (MD), is proposed to indicate the health condition of cooling fan and induction motor based on vibration signal. Anomaly detection and fault classification are accomplished by comparing MDs, which are calculated based on the feature data set extracted from the vibration signals under normal and abnormal conditions. Since MD is a non-negative and non-Gaussian distributed variable, Box–Cox transformation is used to convert the MDs into normal distributed variables, such that the properties of normal distribution can be employed to determine the ranges of MDs corresponding to different health conditions. Experimental data of cooling fan and induction motor are used to validate the proposed approach. The results show that the early stage failure of cooling fan caused by bearing generalized-roughness faults can be detected successfully, and the different unbalanced electrical faults of induction motor can be classified with a higher accuracy by Mahalanobis–Taguchi system. Such works could aid in the reliable operation of the machines, the reduction of the unexpected failures, and the improvement of the maintenance plan.

© 2013 Elsevier Ltd. All rights reserved.

## 1. Introduction

Rotary-machines (such as cooling fans and induction motors) play an important role in modern society. Cooling fans are widely used for thermal management in electronic products. Schroeder and Gibson (2007) reported that cooling fan was one of the top 10 failing components in electronic products. Induction motors, which convert electrical energy into mechanical energy, are the critical component in industrial equipment. Failure of induction motors can lead to their host system breakdowns, loss of production and income, and even casualties (Chow & Hai, 2004; Li, Chow, Tipsuwan, & Hung, 2000; Motor Reliability Working Group, 1985; Thorsen & Dalva, 1999). Therefore, fault diagnosis in these two rotary-machines is important, and plays a key role for the reliable operation of them and their host system, reducing the unexpected failures, and improving the maintenance.

Research on fault diagnosis of rotary-machines has gained increasing interests world-wide, and is still a hot topic today, as evidenced by Prognostics and System Health Management conferences over recent years. Several types of signals are used for this purpose. For examples, acoustic emission signals are analyzed to

estimate the degree of cooling fan bearing degradation (Oh, Azarian, & Pecht, 2011); sound pressure level could differentiate a new and failed cooling fan effectively (Oh, Shibutani, & Pecht, 2012); motor current signals are used to monitor the health condition of induction motor (Niu et al., 2008); and oil-based approaches are used to predict the residual life of plant (Wang, 2009). Although there are many other methods developed for fault diagnosis of rotary machines based on different signals, vibration signal analysis is the most common, effective, and reliable method (Caesarendra, Niu, & Yang, 2010; Chow & Hai, 2004; Gan, Zhao, & Chow, 2009; Randall & Antoni, 2011; Wang, Tse, Guo, & Miao, 2011). Based on vibration signals, the signal processing approaches such as time domain analysis (Heng & Nor, 1998; Martin & Honarvar, 1995), frequency domain analysis (Courrech, 2000; Miao, Cong, & Pecht, 2011; Miao, Azarian, & Pecht, 2011), and time–frequency domain analysis (Tse, Peng, & Yam, 2001; Wang, Zi, & He, 2009), are used for fault diagnosis. In this study, vibration signals from cooling fan and induction motor are also measured and analyzed. Features sets that can reveal the characteristics of time domain and frequency domain of vibration signals are constructed. A health index, Mahalanobis distance (MD), is used and enhanced by Mahalanobis–Taguchi system (MTS) for anomaly detection and fault classification. Then, anomaly detection and fault classification are done by comparing MDs of normal and abnormal conditions.

\* Corresponding author at: Department of Electronic Engineering, City University of Hong Kong, Hong Kong, China. Tel.: +852 34424829; fax: +852 34420272.

E-mail addresses: [xiaohajin2-c@my.cityu.edu.hk](mailto:xiaohajin2-c@my.cityu.edu.hk) (X. Jin), [eetchow@cityu.edu.hk](mailto:eetchow@cityu.edu.hk) (T.W.S. Chow).

MTS combines the MD and Taguchi methods to deal with multivariate problems. It has been successfully applied into different areas, such as damage detection in civil engineering, bankruptcy and financial crisis prediction, and health condition checking (Cheung et al., 2008; Cho, Hong, & Ha, 2010; Lee & Teng, 2009; Taguchi & Jugulum, 2002; Wang, Su, Chen, & Chen, 2011; Yang & Cheng, 2010). Recently, MTS and MD are introduced into fault diagnosis and prognosis of rotary-machines in the following papers: Soylemezoglu, Jagannathan, and Saygin (2011) presented an MTS-based fault diagnosis and prognosis scheme for centrifugal pump failures; Wang, Wang, Tao, and Ma (2012) used MTS to diagnose bearing single-point faults. Jin, Ma, Cheng, and Pecht (2012) presented a health monitoring scheme based on MD with minimum redundancy maximum relevance feature selection. To our best knowledge, it is the first time to use MTS for anomaly detection of cooling fans due to bearings generalized-roughness faults, and fault classification of the unbalanced electrical faults of induction motor.

The main contributions of this paper can be summarized as below: (1) A health index, MD, is proposed to indicate the health condition of cooling fan and induction motor; (2) MTS is employed to make the proposed health index robust; (3) The effectiveness of the proposed health index is validated by two experimental data sets. Results show that early stage of failure of cooling fan caused by bearing generalized-roughness faults can be detected successfully, and different unbalanced electrical faults of induction motor can be classified at a higher accuracy by using MTS.

The rest of this paper is organized as follows. In Section 2, MTS is briefly reviewed, and the way of determination of the ranges of MDs corresponding to different health conditions are introduced. The proposed anomaly detection and fault classification approach is introduced in Section 3. Anomaly detection of cooling fan is reported in Section 4, while fault classification of induction motor is presented in Section 5. Finally, the conclusions are drawn in Section 6.

## 2. Mahalanobis–Taguchi system

MTS is a pattern recognition technology that is widely used for data classification (Taguchi & Jugulum, 2002). It combines the MD and Taguchi methods together. MD is a generalized distance that is useful for determining the similarities between unknown and known sample data sets. It uses a scalar value to represent a multivariate system. Taguchi methods are statistical methods used to improve engineered quality (Taguchi & Jugulum, 2002) and make the system more robust (Taguchi, Chowdhury, & Wu, 2001).

### 2.1. Four steps in MTS

Generally, there are four steps in a MTS, as shown in Fig. 1 (Taguchi & Jugulum, 2002).

#### Step I: Mahalanobis space (MS) construction

Feature data from the healthy products are collected to form the normal data set, and their MDs constitute a reference space that is also known as the MS. Their MDs are around one. In this study, feature data set constructed from the vibration signal from normal rotary machines is used to form the MS.

The normal data set is denoted as  $P$ ;  $p_{ij}$  is the  $i$ th observation on  $j$ th feature, where  $i = 1, 2, \dots, m$ , and  $j = 1, 2, \dots, n$ .  $\bar{P}_j$  and  $S_j$  are the mean and the standard deviation, respectively, of the  $j$ th feature ( $P_j$ ), where  $j = 1, 2, \dots, n$ . Each individual feature in each data vector ( $P_i$ ) is normalized by the mean ( $\bar{P}_j$ ) and the standard deviation ( $S_j$ ). Thus, the normalized values are as follows:

$$z_{ij} = \frac{p_{ij} - \bar{P}_j}{S_j}, \quad i = 1, 2, \dots, m, \quad j = 1, 2, \dots, n \quad (1)$$

where

$$\bar{P}_j = \frac{1}{m} \sum_{i=1}^m p_{ij} \quad (2)$$

$$S_j = \sqrt{\frac{\sum_{i=1}^m (p_{ij} - \bar{P}_j)^2}{m - 1}} \quad (3)$$

The MDs of the normal dataset are calculated using the following equation:

$$MD_i = \frac{1}{n} z_i C^{-1} z_i^T \quad (4)$$

where  $z_i = [z_{i1}, z_{i2}, \dots, z_{in}]$ ,  $z_i^T$  is the transpose vector of  $z_i$ , and  $C^{-1}$  is the inverse of the covariance coefficient matrix  $C$ .  $C$  is calculated as:

$$C = \frac{1}{m - 1} \sum_{i=1}^m z_i^T z_i \quad (5)$$

One issue faced by MD is multicollinearity (strong correlations among features). The problem of multicollinearity will lead to an approximate singular covariance coefficient matrix, an inaccurate inverse matrix of the covariance coefficient matrix, consequently, an inaccurate MD (Taguchi & Jugulum, 2002). MD corresponding to the adjoint matrix of the covariance coefficient matrix, which is denoted as MDA, can be used to handle this problem.

$$MDA_i = \frac{1}{n} z_i C_{adj} z_i^T \quad (6)$$

where  $C_{adj}$  is the adjoint matrix of the covariance coefficient matrix  $C$ . Since  $C^{-1} = C_{adj}/|C|$ , the relationship between MD and MDA is shown as below.

$$MD_i = \frac{1}{|C|} MDA_i \quad (7)$$

#### Step II: Validation of MS

Observations of abnormal conditions are selected out first. Their feature data sets are normalized using the mean and standard deviation of the normal data set. Then their MDs are calculated using the normalized feature data and the covariance coefficient matrix of the normal data set. MDs corresponding to the abnormal conditions will be out of the MS, if the MS is appropriately constructed. In other words, these abnormal conditions associated MDs will have higher values.

#### Step III: Identify the useful features

The useful features are selected out using orthogonal arrays (OAs) and signal-to-noise ratios ( $S/N$  ratios). In MTS, OAs are used to identify the important features by minimizing the different combinations of the original set of features. The number of columns in OA depends on the number of features. Two-level factors are used: Level-1 means including the feature, while Level-2 means excluding the feature.  $S/N$  ratios, which are calculated using abnormal conditions only, are used to measure the accuracy of the MS for predicting. The formula for calculating the  $S/N$  ratio ( $\eta_i$ ) corresponding to the  $i$ th run of the OA is defined as below:

$$\eta_i = -10 \lg \left( \frac{1}{t} \sum_{j=1}^t \frac{1}{MD_j} \right) \quad (8)$$

where  $t$  is the number of abnormal conditions, and  $MD_j$  is the MD of the  $j$ th abnormal condition.

The useful features are obtained by evaluating the “Gain” in S/N ratios. The Gain of each feature is calculated using Eq. (9). Features with positive “Gain” are identified as useful ones.

$$\text{Gain} = \overline{S/N \text{ ratio}}_{\text{Level-1}} - \overline{S/N \text{ ratio}}_{\text{Level-2}} \quad (9)$$

*Step IV: Future diagnosis*

The MS is reconstructed and the MDs of monitored products are calculated by using the useful features identified in Step III. If MDs are within the MS, the monitored products are normal. If MDs are out of the MS, the monitored products exhibit abnormal behaviors. The higher the MDs are, the more deviation between the monitored product and the normal one is.



Fig. 3. Cooling fan and accelerometer (Jin et al., 2012; Miao, Azarian, et al., 2011).

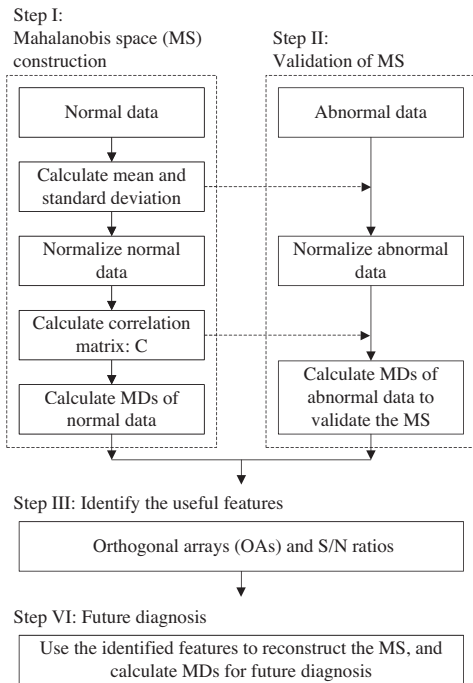


Fig. 1. Four steps in Mahalanobis-Taguchi system.

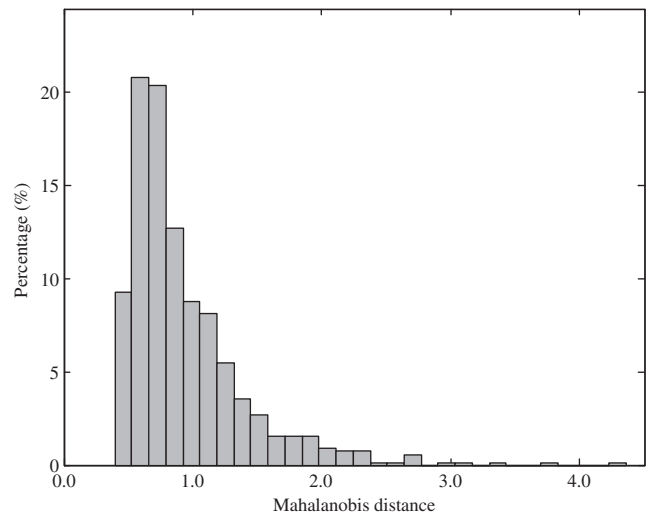


Fig. 4. Histogram of MDs for normal cooling fans.

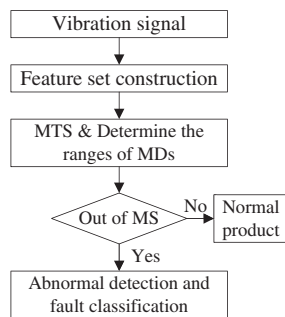


Fig. 2. MD-based anomaly detection and fault classification approach.

Table 1  
Fan ball bearing specifications.

Number of balls, <i>n</i>	Contact angle, $\theta$ (deg)	Pitch diameter of bearing, <i>D</i> (mm)	Ball diameter, <i>d</i> (mm)
6	10.4	5.5	1.59

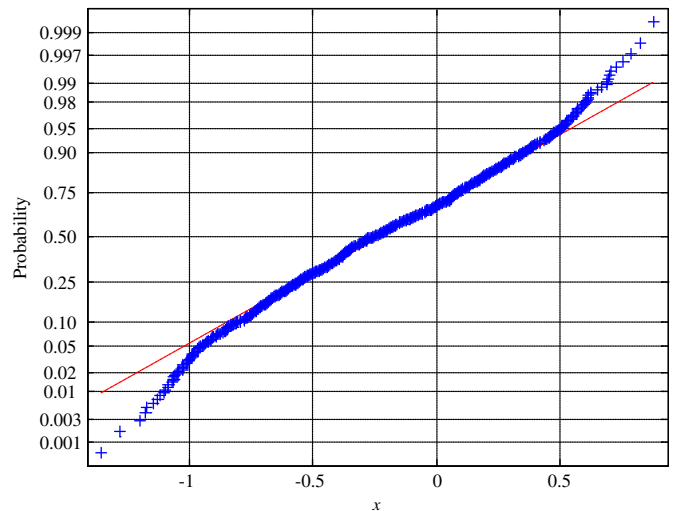


Fig. 5. Normal probability plot of Box-Cox transformed variable *x*.

**Table 2**  
L<sub>16</sub>(2<sup>15</sup>) OA and MDs of three abnormal conditions.

Run	Features													MDs			S/N ratio
	X <sub>1</sub>	X <sub>2</sub>	X <sub>3</sub>	X <sub>4</sub>	X <sub>5</sub>	X <sub>6</sub>	X <sub>7</sub>	X <sub>8</sub>	X <sub>9</sub>	X <sub>10</sub>	X <sub>11</sub>	X <sub>12</sub>	X <sub>13</sub>	1	2	3	
1	1	1	1	1	1	1	1	1	1	1	1	1	1	6487.07	35058.32	40776.12	41.61
2	1	1	1	1	1	1	1	2	2	2	2	2	2	2039.66	7067.49	11520.81	36.21
3	1	1	1	2	2	2	2	1	1	1	1	2	2	2743.70	11511.93	14030.36	37.59
4	1	1	1	2	2	2	2	2	2	2	2	1	1	267.45	2129.94	1288.04	27.79
5	1	2	2	1	1	2	2	1	1	2	2	1	1	1417.17	15839.50	10088.97	35.39
6	1	2	2	1	1	2	2	2	2	1	1	2	2	38.25	387.69	106.93	18.96
7	1	2	2	2	2	1	1	1	1	2	2	2	2	131.50	1577.82	1524.24	25.28
8	1	2	2	2	2	1	1	2	2	1	1	1	1	214.49	270.15	131.47	22.74
9	2	1	2	1	2	1	2	1	2	1	2	1	2	87.31	2232.70	432.39	23.24
10	2	1	2	1	2	1	2	2	1	2	1	2	1	965.55	4003.97	3540.23	32.82
11	2	1	2	2	1	2	1	1	2	1	2	2	1	184.50	4523.82	1230.22	26.67
12	2	1	2	2	1	2	1	2	1	2	1	1	2	1180.04	6749.57	5830.14	34.10
13	2	2	1	1	2	2	1	1	2	2	1	1	2	16.02	464.41	127.78	16.17
14	2	2	1	1	2	2	1	2	1	1	2	2	1	119.59	761.88	438.85	24.00
15	2	2	1	2	1	1	2	1	2	2	1	2	1	124.26	476.17	88.17	21.45
16	2	2	1	2	1	1	2	2	1	1	2	1	2	17.52	273.23	105.20	16.31

**Table 3**  
Average S/N ratios and Gain for each feature.

	X <sub>1</sub>	X <sub>2</sub>	X <sub>3</sub>	X <sub>4</sub>	X <sub>5</sub>	X <sub>6</sub>	X <sub>7</sub>	X <sub>8</sub>	X <sub>9</sub>	X <sub>10</sub>	X <sub>11</sub>	X <sub>12</sub>	X <sub>13</sub>
Level-1	30.70	32.50	27.64	28.55	28.84	27.46	28.35	28.43	30.89	26.39	28.18	27.17	29.06
Level-2	24.34	22.54	27.40	26.49	26.20	27.58	26.69	26.62	24.16	28.65	26.86	27.87	25.98
Gain	6.36	9.96	0.24	2.06	2.64	-0.12	1.66	1.81	6.73	-2.26	1.32	-0.70	3.08

**Table 4**  
Comparison of MDs before and after screening of features.

Fan No.	Time	All features		Features identified by MTS	
		Mean	Range	Mean	Range
#1	0 h	1.00	[0.63,2.26]	1.10	[0.69,2.74]
	8 h	1.17	[0.95,1.41]	1.40	[1.16,1.74]
	16 h	0.63	[0.26,1.48]	0.52	[0.24,1.49]
	24 h	7.59	[3.20,14.97]	6.76	[3.11,10.72]
	48 h	253.37	[161.78,379.10]	155.46	[105.34,220.43]
	72 h	17509.39	[2694.15,72321.73]	17425.39	[2494.33,75758.10]
#2	0 h	0.68	[0.43,1.05]	0.77	[0.54,1.06]
	8 h	5.72	[2.20,11.65]	4.06	[2.39,6.44]
	16 h	21.34	[9.03,35.74]	9.59	[2.88,17.65]
	24 h	2.56	[0.71,5.90]	2.63	[0.83,4.85]
	48 h	3.42	[2.04,5.34]	4.26	[2.58,6.55]
	72 h	36916.99	[18886.76,76503.17]	29195.54	[14597.25,63005.30]
#3	0 h	0.60	[0.46,0.77]	0.76	[0.58,0.98]
	8 h	9.65	[6.74,13.73]	5.51	[3.45,8.08]
	16 h	420.11	[159.65,831.31]	449.61	[187.89,941.13]
	24 h	104.48	[54.43,158.20]	125.78	[67.17,189.14]
	48 h	157.59	[75.41,454.01]	173.79	[94.47,398.90]
	72 h	48568.64	[22221.06,104192.44]	39932.50	[17269.59,87487.38]

2.2. Determine the ranges of MDs

MD is a distance metric with values ranging from zero to infinity. The higher values of MDs are of concern from an abnormal perspective. Generally, they do not follow a normal distribution. To determine the ranges of MDs corresponding to different health conditions of rotary-machines, Box-Cox transformation is employed to transform the non-negative variable, MD, into a normally distributed variable (Box & Cox, 1964). The goodness-of-fit of the transformed variable from the original MDs can be confirmed by plotting them into a normal plot. Considering 95.4% of the data lie within two standard deviations of the mean for a normal distribution, the limits  $\mu \pm 2\sigma$  ( $\mu$  and  $\sigma$  are the mean and standard

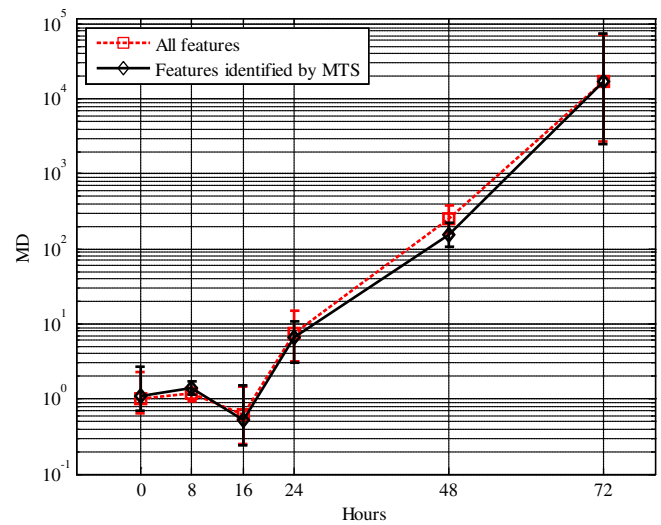


Fig. 6. MDs of Fan #1.

deviation of the transformed variable) are used to determine the limits of the Box-Cox transformed MDs. Since the lower limit of MS is 0,  $\mu + 2\sigma$  is used as the upper limit of transformed threshold of MS. The inverse Box-Cox transformation is then used to calculate the ranges of MDs corresponding to different health conditions, and the threshold of MS.

3. Approach for anomaly detection and fault classification

The proposed anomaly detection and fault classification approach starts with the measurement of the vibration signal as shown in Fig. 2. Both the time domain features and time-frequency domain features are constructed based on the measured vibration

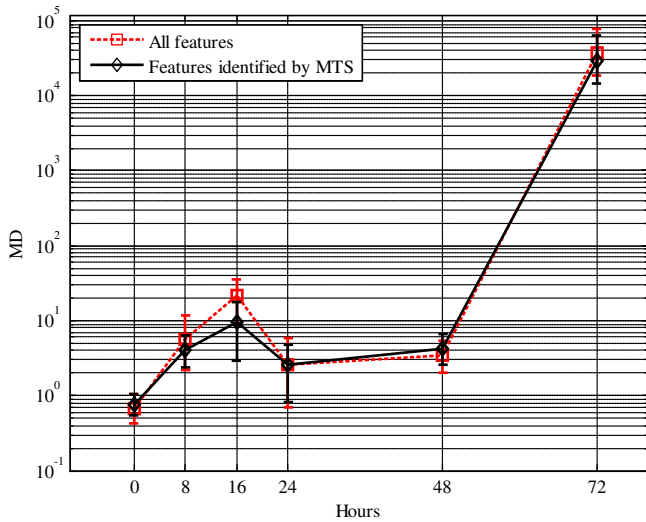


Fig. 7. MDs of Fan #2.

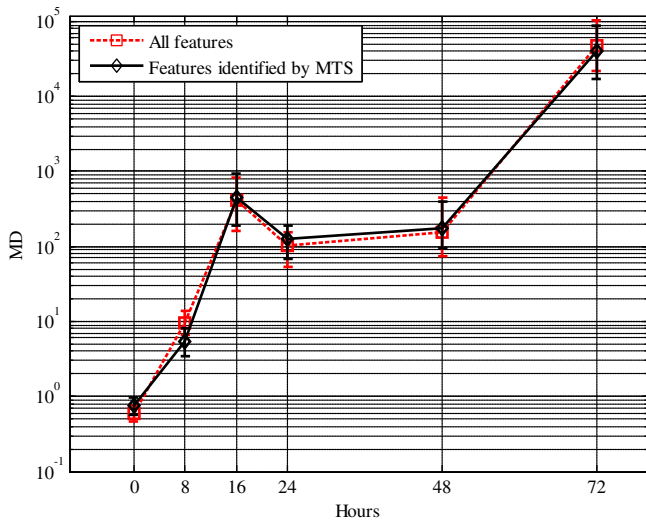


Fig. 8. MDs of Fan #3.

**Table 5**  
Characteristic frequencies of fan ball bearing faults.

Bearing components	Characteristic frequencies (Hz)
Ball passing frequency outer race (BPFO)	$f_{BPFO} = \frac{n}{2}f_r(1 - \frac{d}{D}\cos\theta) = 143.1$
Ball passing frequency inner race (BPFI)	$f_{BPFI} = \frac{n}{2}f_r(1 + \frac{d}{D}\cos\theta) = 256.9$
Ball spin frequency (BSF)	$f_{BSF} = \frac{D}{2d}f_r[1 - (\frac{d}{D}\cos\theta)^2] = 106.0$

signal. The MD corresponding to normal/healthy data, which is called as MS, is constructed and validated. Taguchi methods and signal-to-noise ratios are employed to identify the useful features, and the MDs for normal and different conditions are calculated by using the identified useful features. Anomaly detection is done by comparing MDs with the MS, and fault classification is done by comparing MDs under different health conditions.

When faults occur in rotary-machines, the increased friction, impulsive forces, and unbalanced faults cause both the time domain signal and time–frequency domain signal to deviate from the normal ones. Therefore, a normal rotary-machine and the

rotary-machines with different faults usually have different data distributions in their signals. In this paper, nine statistical features were calculated to represent the vibration signal in the time domain. They were root mean square, peak, skewness, kurtosis, crest factor, clearance factor, shape factor, impact factor, and square mean root. The vibration signals were also decomposed into individual frequency bands by using the algorithm of wavelet packets. Percentages of energy corresponding to wavelet packets coefficients were calculated by decomposing the vibration signal by the wavelet packets transform using “db4” at level 2 (Daubechies, 1988). Thus, thirteen features, which named from  $X_1$  to  $X_{13}$  (including nine time-domain statistical features and four time–frequency domain features), formed the feature data set for fault diagnosis using MTS.

#### 4. Anomaly detection of cooling fan

The analyzed cooling fans data set was collected under high-temperature (70 °C) stress test. Since lubricant plays a critical role in cooling fan ball bearings, lubricant was removed from ball bearing to simulate lubricant starvation (Jin, Azarian, Lau, Cheng, & Pecht, 2011). Ball bearings were NSK 693 ZZ, their geometrical specifications were shown in Table 1. Three cooling fans were made by these customized ball bearings, and were regarded as normal ones before test. A normal cooling fan was also used as a reference. Cooling fan was mounted on a test plenum, powered by a 12 V DC power supply, and controlled by a pulse width modulation signal (duty cycle was set at 74%) for data acquisition. The rotation speed of the fan was 4000 rpm, corresponding to the rotation frequency,  $f_r$ , of 66.7 Hz. A PCB accelerometer was used to acquire the vibration signal, as shown in Fig. 3. After the three tailor-made cooling fans underwent 0-, 8-, 16-, 24-, 48-, and 72-h high-temperature stress tests, their vibration signals and the vibration signal from the normal cooling fan were measured. The sampling rate was set at 102.4 kHz. The high-temperature stress test was stopped when cooling fan’s sound pressure level (SPL) increased more than 3 dBA from the initial value, which is one of the failure criteria for cooling fan defined in IPC-9591 (2006).

Feature data sets from the normal cooling fans (including the referenced normal cooling fan and the three tailor-made cooling fans at 0-h) were used to form the MS. The MDs of normal cooling fans were around one; however, they did not follow a normal distribution, as shown in Fig. 4. Box–Cox transformation with the parameter  $\lambda$  at an optimized value of  $-0.77$  was used to transform the MDs into a normal distributed variable with a mean of  $-0.24$  and a standard deviation of 0.43. The normal probability plot of the transformed variable is shown in Fig. 5. The threshold of the transformed MDs was set as 0.62, which corresponds to the untransformed MD of 2.37. Therefore, the MS of these cooling fans is the MDs that range from 0 to 2.37.

All three tailor-made cooling fans failed after they underwent 72-h high-temperature stress tests, since their SPLs increased more than 3 dBA from the initial values. The vibration signals of the three cooling fans at 72 h were used to validate the measurement scale, MS, in Step II of MTS and identify the useful features in Step III. The failed cooling fan data were normalized using the mean and standard deviations of the normal cooling fans. Their MDs were calculated using the covariance coefficient matrix of the normal cooling fans and were 6487.07, 35058.32, and 40776.12, respectively. They were clearly out of the MS. Hence, the MS is validated.

In Step III of MTS, the impact of each feature was investigated using OAs and  $S/N$  ratios. The Gain of each feature was calculated for three abnormal conditions of cooling fans. Since 13 features was constructed, a  $L_{16}(2^{15})$  OA was used. As shown in Tables 2 and 3,  $X_6$ ,  $X_{10}$ , and  $X_{12}$  did not have a significant impact on MD.

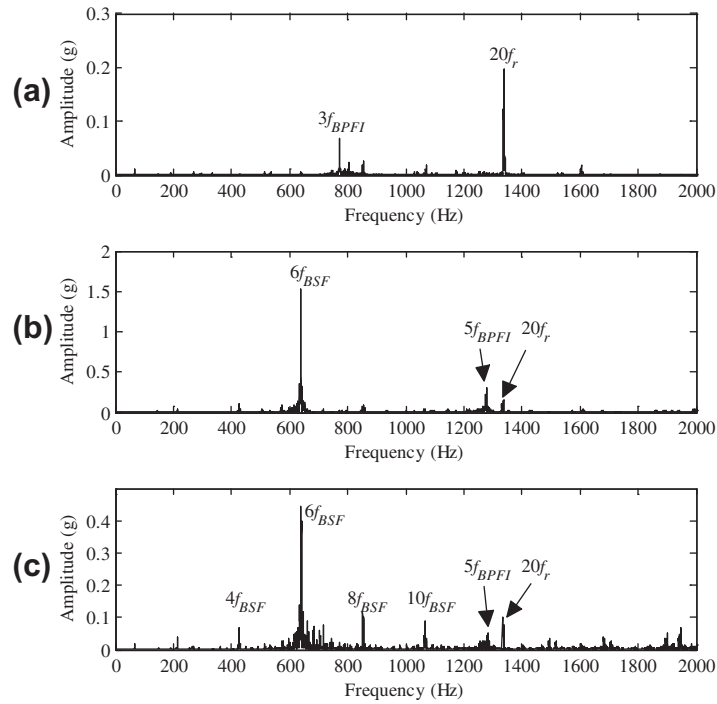


Fig. 9. Frequency spectrum of the three cooling fans at 72-h (a) Fan #1 (b) Fan #2 (c) Fan #3.

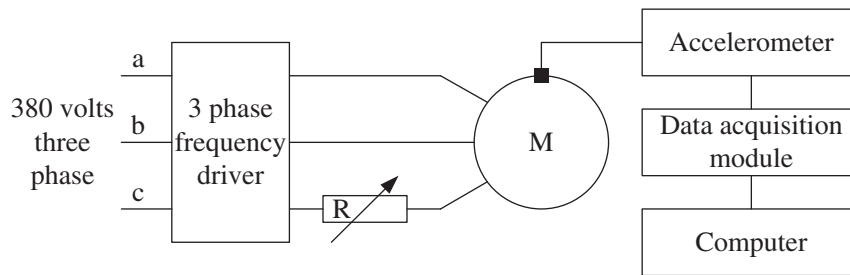


Fig. 10. Schematic of induction motor test rig.

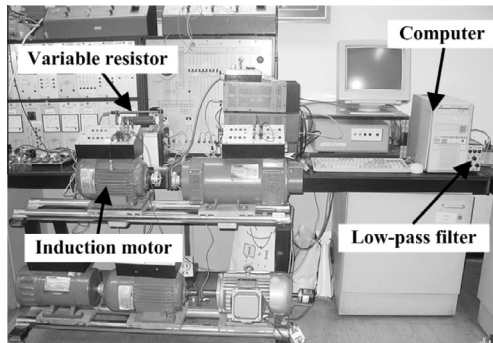


Fig. 11. Experimental setup and data acquisition system.

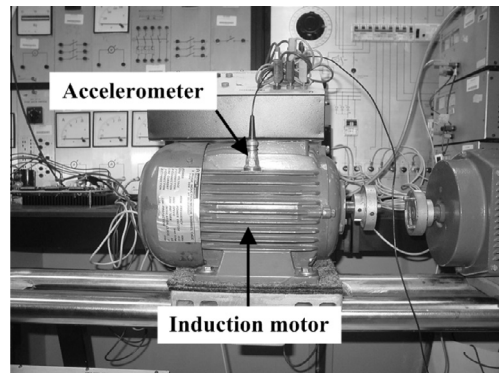


Fig. 12. Induction motor and accelerometer.

Therefore, the number of features was reduced from 13 to 10. The MDs and threshold of MS were recalculated using the identified useful features. The revised threshold of the MS of the fans was 2.35. MDs of the three fans after they underwent 8-, 16-, 24-, 48- and 72-h high-temperature stress tests using all features, and the useful features identified by MTS, are shown and compared in Table 4 and Figs. 6–8. The failed cooling fans at 72-h could be clearly distinguished from the normal fans, since their MDs (ranging from 2494.33 to 87487.38) deviated greatly from the MS. Although there

is little change of mean and range of MDs, which were calculated by the useful features identified by MTS, compared with original ones, multicollinearity issue faced by MD was solved, thereby, making the proposed approach for anomaly detection more robust.

The deviations of MDs at 72-h among the three fans were large. This was due to the fact that the cooling fan bearings had different prominent failure modes and different degrees of failure. Referring to the bearing characteristic frequencies in Table 5 and the 72-h

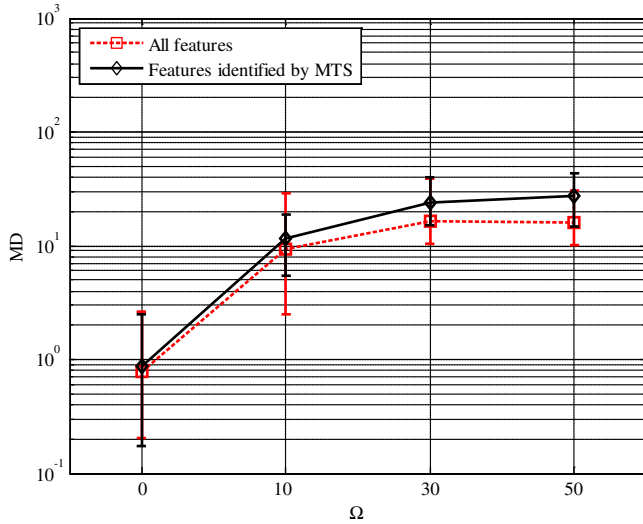


Fig. 13. MDs of induction motor under different unbalanced electrical faults at supply frequency 40 Hz.

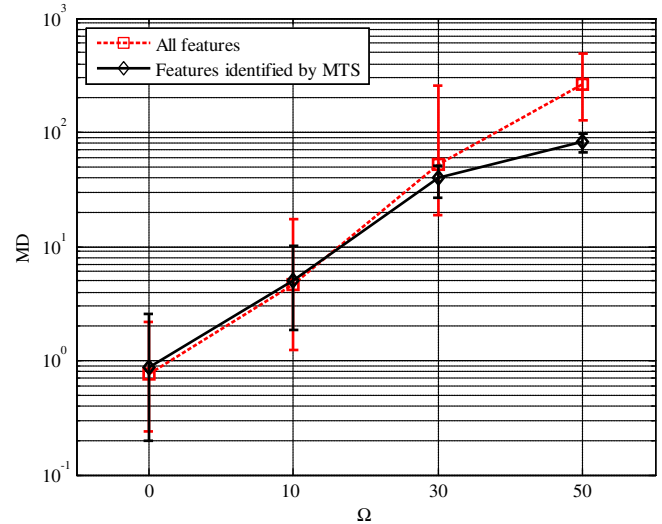


Fig. 15. MDs of induction motor under different unbalanced electrical faults at supply frequency 50 Hz.

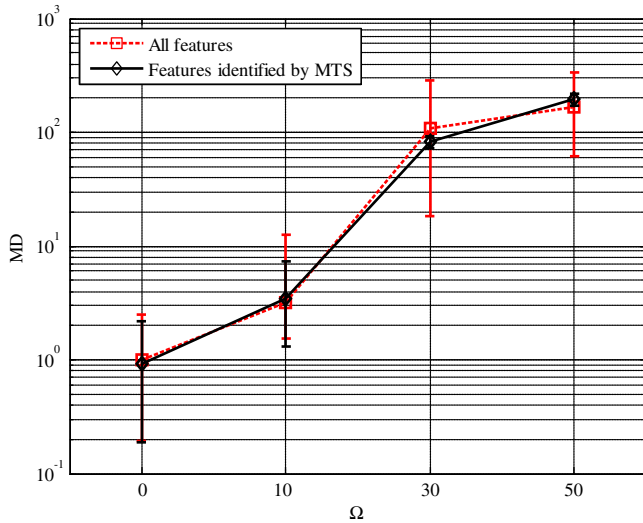


Fig. 14. MDs of induction motor under different unbalanced electrical faults at supply frequency 45 Hz.

frequency spectrum of vibration signals in Fig. 9, the prominent failure mode in Fan #1 is the inner race of the ball bearing, while the prominent failure modes in Fan #2 and Fan #3 are ball failure. The degrees of the ball failures in Fan #2 and Fan #3 are also different.

As shown in Table 4 and Figs. 6–8, MDs of Fan #1 at 24-h, and MDs of Fan #2 and Fan #3 at 8-h are out of MS. Therefore, the proposed method could detect the incipient bearing defects of the cooling fans. An increased trend in the average of MDs could also be found; however, they fluctuated. The natural failure process could explain these fluctuating symptoms. When cooling fan bearings degraded due to the lack of lubricant, the increasing friction damaged the surfaces of the bearings and resulted in small pieces of metal dropping off. The dropped metal and the defective bearing surface were ground smoothly by the continuous operation of the cooling fan bearings. Hence, the vibration signals became weaker. However, as the defects grew, the vibration became stronger leading to the larger MDs, and caused cooling fans to emit abnormal sounds in the end.

### 5. Fault classification of induction motor

Unbalanced electrical faults of a three-phase induction motor were used in this section to demonstrate the effectiveness of the proposed MD-based method for fault classification. In order to simulate the unbalanced electrical faults in a three-phase induction motor, a noninvasive test rig as shown in Fig. 10 was used. The detection of induction motor unbalance electrical faults was based on the stator core vibration signals. The data acquisition system was shown in Fig. 11. The rated power and speed of the induction motor were 1100 W and 1440 r/min, respectively. Three cases at different rotation speeds were studied. These were obtained by feeding the motor with different supply frequencies at 40, 45, and 50 Hz, respectively. Induction motor was driven under different asymmetrical faults by setting different values of the variable resistor at 10, 30, and 50 Ω, respectively, at three rotation speeds each. The vibration signal was measured by an accelerometer mounted on the induction motor as shown in Figs. 11 and 12.

Feature data sets from the normal induction motor were used to form the referenced space, MS. MDs of normal induction motors range from 0 to 2.43 calculated by the methods introduced in Section 2.2. Three vibration signals of the induction motor unbalanced electrical faults were used to validate the MS. The induction motor fault data were normalized by the mean and standard deviations of the normal induction motor. Their MDs, which were calculated using the covariance coefficient matrix of the normal induction motor, are 4.59, 59.48, and 148.31. They are out of the MS. Hence, the MS is validated.

MDs corresponding to induction motor's unbalanced electrical faults at different rotation speeds are shown in Figs. 13–15. In Fig. 13, MDs at 10 Ω overlap with MDs at 30 Ω heavily; an increasing trend in the MDs representing the increasing degree of faults in rotary machines could not be observed, since the ranges of MDs at 30 Ω included MDs at 50 Ω, and a decreasing trend is shown by their means. An increasing trend in MDs is shown in Figs. 14 and 15, however, MDs corresponding to different conditions are heavily overlapped. Therefore, Taguchi methods were employed to investigate the impact of each feature. Since the number of constructed features was 13, a  $L_{16}(2^{15})$  OA was used. The 'Gain' of each feature was calculated under three unbalanced electrical faults conditions of the induction motor. As shown in Tables 6 and 7,  $X_2, X_3, X_4, X_5, X_8, X_9, X_{11},$  and  $X_{12}$  do not have a significant impact on MD. Hence, the number of features was reduced from 13 to 5.

**Table 6**  
 $L_{16}(2^{15})$  OA and MDs of three abnormal conditions.

Run	Features													MDs			S/N ratio
	$X_1$	$X_2$	$X_3$	$X_4$	$X_5$	$X_6$	$X_7$	$X_8$	$X_9$	$X_{10}$	$X_{11}$	$X_{12}$	$X_{13}$	1	2	3	
1	1	1	1	1	1	1	1	1	1	1	1	1	1	4.59	59.48	148.31	10.95
2	1	1	1	1	1	1	1	2	2	2	2	2	2	6.54	54.11	71.75	12.09
3	1	1	1	2	2	2	2	1	1	1	2	2	2	4.25	63.02	141.51	10.65
4	1	1	1	2	2	2	2	2	2	2	2	1	1	6.08	96.68	236.60	12.24
5	1	2	2	1	1	2	2	1	1	2	2	1	1	4.25	69.72	171.96	10.70
6	1	2	2	1	1	2	2	2	2	1	1	2	2	4.82	81.78	175.99	11.24
7	1	2	2	2	2	1	1	1	1	2	2	2	2	7.34	48.91	152.62	12.64
8	1	2	2	2	2	1	1	2	2	1	1	1	1	6.46	69.13	142.50	12.31
9	2	1	2	1	2	1	2	1	2	1	2	1	2	3.34	78.06	195.40	9.76
10	2	1	2	1	2	1	2	2	1	2	1	2	1	4.02	56.69	80.64	10.32
11	2	1	2	2	1	2	1	1	2	1	2	2	1	5.12	63.40	149.53	11.39
12	2	1	2	2	1	2	1	2	1	2	1	1	2	2.81	74.72	193.52	9.04
13	2	2	1	1	2	2	1	1	2	2	1	1	2	2.26	46.59	120.18	8.02
14	2	2	1	1	2	2	1	2	1	1	2	2	1	5.06	62.35	139.42	11.33
15	2	2	1	2	1	1	2	1	2	2	1	2	1	5.10	30.36	68.63	10.90
16	2	2	1	2	1	1	2	2	1	1	2	1	2	3.58	78.08	183.91	10.04

**Table 7**  
 Average S/N ratios and Gain for each feature.

	$X_1$	$X_2$	$X_3$	$X_4$	$X_5$	$X_6$	$X_7$	$X_8$	$X_9$	$X_{10}$	$X_{11}$	$X_{12}$	$X_{13}$
Level-1	11.60	10.81	10.78	10.55	10.79	11.13	10.97	10.63	10.71	10.96	10.43	10.38	11.27
Level-2	10.10	10.90	10.92	11.15	10.91	10.58	10.73	11.08	11.00	10.74	11.27	11.32	10.44
Gain	1.50	-0.09	-0.14	-0.60	-0.12	0.55	0.24	-0.45	-0.29	0.22	-0.84	-0.94	0.83

**Table 8**  
 Induction motor unbalanced electrical faults classification accuracy.

Supply frequency (Hz)	Unbalanced electrical faults ( $\Omega$ )	Original MDs (%)	MTS MDs (%)
40	10	53.33	83.33
	30	10.00	80.00
	50	0.00	10.00
45	10	63.33	83.33
	30	26.67	100.00
	50	3.33	100.00
50	10	83.33	93.33
	30	90.00	100.00
	50	46.67	100.00

The MDs and MS were recalculated using the identified useful features by MTS. MDs were transformed into a normal distributed variable using Box-Cox transformation. Properties of normal distribution were used to determine the ranges of MDs corresponding to each fault. The revised threshold of MS is 2.42. MDs of normal induction motor and induction motor with different faults using all features and useful features identified MTS were shown and compared in Figs. 13–15. By narrowing most ranges of MD distributions using MTS, different faults could be distinguished easily except faults at 50  $\Omega$  with supply frequency at 40 Hz, thereby improving the performance of MD-based approach for fault classification. Table 8 shows the classification performance using original MDs and MDs enhanced by MTS. MDs enhanced by MTS achieved the better performance. These results verified the effectiveness of the proposed approach for fault classification of induction motor's unbalanced electrical faults.

## 6. Conclusion

In this paper, a health index, MD, was proposed to indicate the health condition of cooling fan and induction motor. Anomaly detection of cooling fan and fault classification of induction motor were accomplished by constructing feature data set from the vibration signal and comparing MDs corresponding to different health

conditions. MD is a distance metric with values ranging from zero to infinity; however, it does not follow a normal distribution. Box-Cox transformation and properties of normal distribution were used to determine the ranges of MDs. MDs were enhanced by Taguchi methods and signal-to-noise ratios to identify the useful features, for anomaly detection and fault classification. If the MDs are small and within the MS, their corresponding rotary-machines are normal/healthy. If the MDs are larger, and out of the MS, indicating that faults or incipient faults have occurred. The more defects the rotary-machines have, the larger the MD is.

Cooling fan and induction motor experimental data were employed to validate the proposed approach. The experimental results showed that MDs corresponding to failed rotary-machines deviated greatly from the normal ones. An increasing trend in the MDs represented the increasing degree of faults in rotary-machines. Therefore, MDs can indicate the severity of the fault. The results also show that early stage of failure of cooling fan caused by bearing generalized-roughness faults can be detected successfully and different conditions of induction motor due to unbalanced electrical faults could be classified at a higher accuracy by MTS. Future work includes health monitoring the ongoing condition of rotary-machines and predicting machines future state based on the proposed index, MD, to aid in decision-making and allow for the avoidance of unscheduled maintenance and the reduction of economic losses.

## Acknowledgment

The authors would like to thank Dr. Eden W.M. Ma and the anonymous reviewers for helpful and insightful comments and suggestions. The authors would also like to thank the Center for Advanced Life Cycle Engineering, University of Maryland, College Park, for providing the cooling fan data. The work described in this paper was partially supported by a Grant from the Research Grants Council of the Hong Kong Special Administrative Region, China (CityU8/CRF/09) and the City University Strategic Research Grants (7002914).

## References

- Box, G., & Cox, D. (1964). An analysis of transformations. *Journal of the Royal Statistical Society Series B (Methodological)*, 26(2), 211–252.
- Caesarendra, W., Niu, G., & Yang, B. S. (2010). Machine condition prognosis based on sequential Monte Carlo method. *Expert Systems with Applications*, 37(3), 2412–2420.
- Cheung, A., Cabrera, C., Sarabandi, P., Nair, K. K., Kiremidjian, A., & Wenzel, H. (2008). The application of statistical pattern recognition methods for damage detection to field data. *Smart Materials and Structures*, 17(6), 065023.
- Cho, S., Hong, H., & Ha, B. C. (2010). A hybrid approach based on the combination of variable selection using decision trees and case-based reasoning using the Mahalanobis distance: For bankruptcy prediction. *Expert Systems with Applications*, 37(4), 3482–3488.
- Chow, T. W. S., & Hai, S. (2004). Induction machine fault diagnostic analysis with wavelet technique. *IEEE Transactions on Industrial Electronics*, 51(3), 558–565.
- Courrech, J. (2000). Envelope analysis for effective rolling-element fault detection—fact or fiction? *Up Time Magazine*, 8, 14–17.
- Daubechies, J. (1988). Orthonormal bases of compact supported wavelets. *Communications on Pure and Applied Mathematics*, 41(7), 909–996.
- Gan, Z., Zhao, M. B., & Chow, T. W. S. (2009). Induction machine fault detection using clone selection programming. *Expert Systems with Applications*, 36(4), 8000–8012.
- Heng, R. B. W., & Nor, M. J. M. (1998). Statistical analysis of sound and vibration signals for monitoring rolling element bearing condition. *Applied Acoustics*, 53(1), 211–226.
- IPC-9591. (2006). Performance parameters (mechanical, electrical, environmental and quality/reliability) for air moving devices. IPC.
- Jin, X., Azarian, M. H., Lau, C., Cheng, L. L., & Pecht, M. (2011). Physics-of-failure analysis of cooling fans. In *IEEE international conference on prognostics and system health management*. Shenzhen, China.
- Jin, X., Ma, E. W. M., Cheng, L. L., & Pecht, M. (2012). Health monitoring of cooling fans based on Mahalanobis distance with mRMR feature selection. *IEEE Transactions on Instrumentation and Measurement*, 61(8), 2222–2229.
- Lee, Y. C., & Teng, H. L. (2009). Predicting the financial crisis by Mahalanobis–Taguchi system – Examples of Taiwan’s electronic sector. *Expert Systems with Applications*, 36(4), 7469–7478.
- Li, B., Chow, M. Y., Tipsuwan, Y., & Hung, J. C. (2000). Neural-network-based motor rolling bearing fault diagnosis. *IEEE Transactions on Industrial Electronics*, 47(5), 1060–1069.
- Martin, H. R., & Honarvar, F. (1995). Application of statistical moments to bearing failure detection. *Applied Acoustics*, 44(1), 67–77.
- Miao, Q., Cong, L., & Pecht, M. (2011). Identification of multiple characteristic components with high accuracy and resolution using the zoom interpolated discrete Fourier transform. *Measurement Science and Technology*, 22(5), 055701.
- Miao, Q., Azarian, M., & Pecht, M. (2011). Cooling fan bearing fault identification using vibration measurement. In *IEEE international prognostics and health management conference*. Denver, CO, USA.
- Motor Reliability Working Group (1985). Report of large motor reliability survey of industrial and commercial installations, Part I. *IEEE Transactions on Industry Applications*, 21(4), 853–864.
- Niu, G., Widodo, A., Son, J. D., Yang, B. S., Hwang, D. H., & Kang, D. S. (2008). Decision-level fusion based on wavelet decomposition for induction motor fault diagnosis using transient current signal. *Expert Systems with Applications*, 35(3), 918–928.
- Oh, H., Azarian, M., & Pecht, M. (2011). Estimation of fan bearing degradation using acoustic emission analysis and Mahalanobis distance. In *Proceeding of the applied system health management conference*.
- Oh, H., Shibutani, T., & Pecht, M. (2012). Precursor monitoring approach for reliability assessment of cooling fans. *Journal of Intelligent Manufacturing*, 23(2), 173–178.
- Randall, R. B., & Antoni, J. (2011). Rolling element bearing diagnostics – A tutorial. *Mechanical Systems and Signal Processing*, 25(2), 485–520.
- Schroeder, B., & Gibson, G. A. (2007). Understanding disk failure rates: What does an MTTF of 1,000,000 hours mean to you? *ACM Transactions on Storage*, 3(3), 8es.
- Soylemezoglu, A., Jagannathan, S., & Saygin, C. (2011). Mahalanobis–Taguchi system as a multi-sensor based decision making prognostics tool for centrifugal pump failures. *IEEE Transactions on Reliability*, 60(4), 864–878.
- Taguchi, G., Chowdhury, S., & Wu, Y. (2001). *The Mahalanobis–Taguchi system*. McGraw-Hill.
- Taguchi, G., & Jugulum, R. (2002). *The Mahalanobis–Taguchi strategy—a pattern technology system*. John Wiley and Sons.
- Thorsen, O. V., & Dalva, M. (1999). Failure identification and analysis for high-voltage induction motors in the petrochemical industry. *IEEE Transactions on Industry Applications*, 35(4), 810–818.
- Tse, P. W., Peng, Y. H., & Yam, R. (2001). Wavelet analysis and envelope detection for rolling element bearing fault diagnosis – Their effectiveness and flexibilities. *Journal of Vibration and Acoustics*, 123, 303–310.
- Wang, W. (2009). Plant residual time modeling based on observed variables in oil samples. *Journal of the Operational Research Society*, 60, 789–796.
- Wang, Z., Wang, Z., Tao, L., & Ma, J. (2012). Fault diagnosis for bearing based on Mahalanobis–Taguchi system. In *IEEE international conference on prognostics and system health management*. Beijing, China.
- Wang, P. C., Su, C. T., Chen, K. H., & Chen, N. H. (2011). The application of rough set and Mahalanobis distance to enhance the quality of OSA diagnosis. *Expert Systems with Applications*, 38(6), 7828–7836.
- Wang, D., Tse, P. W., Guo, W., & Miao, Q. (2011). Support vector data description for fusion of multiple health indicators for enhancing gearbox fault diagnosis and prognosis. *Measurement Science and Technology*, 22, 025102.
- Wang, X., Zi, Y., & He, Z. (2009). Multiwavelet construction via an adaptive symmetric lifting scheme and its applications for rotating machinery fault diagnosis. *Measurement Science and Technology*, 20(4), 045103.
- Yang, T., & Cheng, Y. T. (2010). The use of Mahalanobis–Taguchi system to improve flip-chip bumping height inspection efficiency. *Microelectronics Reliability*, 50(3), 407–414.